Title

Macrophage Syk—PI3Kγ Inhibits Antitumor Immunity: SRX3207, a Novel Dual Syk—PI3K Inhibitory Chemotype Relieves Tumor Immunosuppression

Journal

Molecular Cancer Therapeutics, 19(3)

ISSN

1535-7163

Authors

Joshi, Shweta
Liu, Kevin X
Zulcic, Muamera
et al.

Publication Date

2020-03-01

DOI

10.1158/1535-7163.mct-19-0947

Peer reviewed

HHS Public Access

Author manuscript

Mol Cancer Ther. Author manuscript; available in PMC 2020 September 01.

Published in final edited form as:

Mol Cancer Ther. 2020 March ; 19(3): 755–764. doi:10.1158/1535-7163.MCT-19-0947.

Macrophage Syk-PI3Kγ inhibits anti-tumor immunity: SRX3207, a novel dual Syk-PI3K inhibitory chemotype relieves tumor immunosuppression

Shweta Joshi[a,*], **Kevin X. Liu**[a], **Muamera Zulcic**[a], **Alok R. Singh**[a], **Dylan Skola**[b], **Christopher K. Glass**[b], **P. Dominick Sanders**[c], **Andrew B. Sharabi**[c], **Timothy V. Pham**[a,d], **Pablo Tamayo**[d], **Daniel Shiang**[a], **Huy Q. Dinh**[e], **Catherine C. Hedrick**[e], **Guillermo A. Morales**[f], **Joseph R. Garlich**[f], **Donald L. Durden**[a,f,*]

[a]UCSD Department of Pediatrics, University of California, San Diego, USA

[b]UCSD School of Medicine, University of California, San Diego, USA

[c]Moores Cancer Center, Department of Radiation Medicine and Applied Sciences, University of California, San Diego, USA

[d]Office of Cancer genomics, University of California San Diego, USA

[e]La Jolla Institute of Allergy and Immunology, La Jolla, CA, USA

[f]SignalRx Pharmaceuticals, Omaha, NE, USA

Abstract

Macrophages (MΦ) play a critical role in tumor growth, immunosuppression and inhibition of adaptive immune responses in cancer. Hence, targeting signaling pathways in MΦs that promote tumor immunosuppression will provide therapeutic benefit. PI3Kγ has been recently established by our group and others as a novel immuno-oncology target. Herein, we report that a macrophage Syk-PI3K axis drives polarization of immunosuppressive MΦs which establish an immunosuppressive tumor microenvironment in *in vivo* syngeneic tumor models. Genetic or pharmacological inhibition of Syk and/or PI3Kγ in MΦs promotes a pro-inflammatory MΦ

Corresponding authors: Shweta Joshi, Moores Cancer Center, University of California San Diego, 3855 Health Sciences Drive, San Diego, CA 92093. Phone: 858-822-7580; shjoshi@ucsd.edu; Donald L. Durden, ddurden@ucsd.edu, Phone: (858) 534-3355.
*These authors contributed equally to the work.

Author Contributions:

Conception and design: S. Joshi., K. Liu., A.R. Singh, D. Durden, A. Sharabi, C. Hedrick and C. Glass.

Development of methodology: S. Joshi., K. Liu., A.R. Singh, D. Shiang., H. Dinh, M. Zulcic, P.D. Sanders, D. Durden, A. Sharabi, C. Hedrick and C. Glass.

Acquisition of data (provided animals, acquired and managed patients, provided facilities, etc.) S. Joshi, D. Durden, G. Morales, J. Garlich, A. Sharabi, C. Hedrick and C. Glass

Analysis and interpretation of data (e.g., statistical analysis, biostatistics, computational analysis): S. Joshi, H. Dinh, T. Pham, P. Tamayo, D. Skola, C. Glass, D. Durden.

Writing, review, and/or revision of the manuscript: S. Joshi, K. Liu, D. Durden, G. Morales, J. Garlich, A. Sharabi, C. Glass.

Administrative, technical, or material support (i.e., reporting or organizing data, constructing databases): D. Skola, T. Pham, P. Tamayo.

Study supervision: S. Joshi, D. Durden

Disclosure of potential conflict of interest

J.R.G., G.A.M., and D.L.D. are consultants of SignalRx Pharmaceuticals and have financial conflicts of interest regarding the SRX3188 and SRX3207 compounds under study in this manuscript. DLD is founder, member of the board and has an equity position in this company.

phenotype, restores CD8+ T cell activity, destabilizes HIF under hypoxia, and stimulates an antitumor immune response. Assay for Transposase-accessible Chromatin using Sequencing (ATAC-seq) analyses on the bone marrow derived macrophages (BMDMs) show that inhibition of Syk kinase promotes activation and binding of NF-κB motif in $Syk^{MC\text{-}KO}$ BMDMs, thus stimulating immunostimulatory transcriptional programming in MΦs to suppress tumor growth. Finally, we have developed *in silico* the "first in class" dual Syk/PI3K inhibitor, SRX3207, for the combinatorial inhibition of Syk and PI3K in one small molecule. This chemotype demonstrates efficacy in multiple tumor models and represents a novel combinatorial approach to activate antitumor immunity.

Keywords

Macrophage; T cells; immune suppression; Syk; HIFα; adaptive immunity

Introduction

Macrophages (MΦs) play a broad role in host defense but can also serve as major drivers of tumor growth, metastasis, and immunosuppression, observed in the tumor microenvironment (TME) (1,2). In response to various environmental signals produced by tumor and stromal cells, proinflammatory MΦs shift to immunosuppressive phenotype that block anti-tumor immunity (3). Hence, targeting the molecular pathways/signaling nodes in the MΦs that regulate transition of pro-tumorigenic MΦs into anti-tumorigenic MΦs will activate immune response in cancer. Although recent studies shed some light on the molecular entities involved in the activation of protumorigenic MΦs (4–6), the identification of potential druggable targets and small molecules to control MΦ immunosuppression of antitumor immunity are still needed.

Syk kinase is a well-established cytoplasmic protein tyrosine kinase implicated in inflammation and hematopoietic cell responses including integrin and immunoreceptor tyrosine activation motif (ITAM) signaling (7–9). As a modulator of tumorigenesis, the role of Syk is highly controversial, it acts as tumor promoter in some cancers (10,11), and in others it is tumor suppressor (12,13). Syk kinase has been extensively studied in adaptive immune responses, but its role in MΦ-mediated innate immune responses remains unclear (14). Previous studies by our group revealed Syk kinase as a novel component of $\alpha_4\beta_1$ integrin-Rac2 signaling axis that encodes myeloid and endothelial Rac2 specificity *in vivo* (8,15). Within the TME, Syk kinase functions upstream of Rac2 GTPase and PI3K to modulate integrin ($\alpha_v\beta_3/\alpha_v\beta_5\&\alpha_4\beta_1$)-mediated migration and metastasis *in vivo* (16) *a*nd these reports suggest a role for Syk kinase in regulating MΦ polarization and immunosuppression.

Another target for negative regulation of anti-tumor immunity recently discovered and reported by our group and other labs is the PI3K signaling pathway, in particular p110γ in MΦs (6,17). Our lab has reported that p110γ in MΦs promotes expression of pro-tumorigenic MΦs in TME and our pan PI3K/BRD4 inhibitor SF1126 or SF2523, blocked tumor growth and macrophage mediated immunosuppression in tumors (17,18).

Furthermore, Syk kinase is required for activation of PI3K in MΦs and B cells (19,20). These reports lead us to propose a hypothesis, that targeting two crucial signaling entities that promote MΦ-mediated immunosuppression viz. Syk kinase and PI3K will activate the anti-tumor immune response. With this aim, using computational chemistry methods, our lab has developed a novel chemotype, SRX3207 that inhibits both PI3K and Syk, with a single molecule for maximal activation of adaptive immune responses.

In this manuscript, using a genetic approach and pharmacological blockade, we provide evidence that Syk kinase plays a crucial role in the control of macrophage-mediated immune suppression and the inhibition of anti-tumor immunity. Moreover, our novel dual inhibitory chemotype, SRX3207 blocks both PI3K and Syk in MΦs thereby activating innate and adaptive antitumor immunity *in vivo*.

Materials and Methods

Mice, murine macrophages and hypoxia experiments

All procedures involving animals were approved by the UCSD Animal Care Committee, which serves to ensure that all federal guidelines concerning animal experimentation are met. Floxed Syk mice and lysozyme M (LysM) Cre recombinase transgenic mice were purchased from Jackson laboratories. Integrin α4Y991A mice and normal littermates in C57BL/6J genetic background have been described before (16,21). BMDMs were isolated as described previously (16). For hypoxia experiments, MΘs were placed in a modulator incubator chamber (Billups-Rothenberg) as described before (16).

In vivo tumor experiments

LLC, B16 melanoma and CT26 cells were obtained from the American Type Culture Collection (ATCC) and were cultured in DMEM or RPMI media containing 10% FBS. B16-OVA cells were obtained from Dr. Andrew Sharabi. All cell lines were tested for mycoplasma and mouse pathogens and checked for authenticity against the International Cell Line Authentication Committee (ICLAC; http://iclac.org/databases/cross-contaminations/) list. LLC or B16 or B16-OVA or CT26 (1×10^5) cells were injected subcutaneously into syngeneic mice and were treated with 40 mg/kg R788 administered orally or 10mg/kg IPI549 or SRX3207 orally, starting from day 10 when tumors reached $100mm^3$ until tumors were harvested on day 21. In another experiment, B16-OVA cells were injected in C57BL/6 WT mice and when tumors reached 100 mm^3, mice were treated with 200μg anti-PDL1 antibodies either alone or in combination with 40 mg/kg R788 as described in supplementary methods. CD8 depletion and macrophage depletion experiments were performed as described earlier (18) and in supplementary methods.

Isolation of single cells from tumors, flow cytometry and mass cytometry

Tumors were isolated, minced and then enzymatically dissociated in collagenase digestion cocktail at 37°C for 30–45 min and cells were prepared for magnetic bead purification of CD11b, or CD90.2 cells or for flow cytometry as reported before (16,18). For mass cytometry, cells were subsequently stained with metal labeled antibodies cocktail and run on mass cytometer (CyTOF, Fluidigm) as described in supplementary methods.

Quantification of gene expression and RNA sequencing.—Total RNA was isolated from BMDMs and TAMs using the Qiagen RNAeasy kit (Qiagen, Hilden, Germany) and cDNA was amplified by RTPCR as described before (16). For RNA sequencing, RNA libraries were prepared and sequenced on Illumina HiSeq2000 using standard Illumina protocols described in supplementary methods.

ATAC-seq.—To profile open chromatin, ATAC-seq was performed on LPS and IL4 stimulated BMDMs. The cells were submitted to UCSD Center for Epigenomics. The details are available in Supplementary methods.

Molecular modeling and *in silico* design, optimization, synthesis and PK/PD of SRX3188 and SRX3207 chemotypes.—X-ray structures of human Syk, ZAP70 and PI3K/p110α and PI3K/p110γ (PDB codes: 4XG9, 1U59, 4JPS and 4XZ4, respectively) were obtained from the Protein Data Bank. Detailed description of *in silico* design of SRX3188 and SRX3207 are provided in supplementary methods. Detailed description of synthesis of SRX3188 and SRX3207 has been described before, where compound 1 and 3 refers to SRX3188 and SRX3207 respectively (22). PK/PD and ADME properties of the compounds were studied in collaboration with Quintara Discovery (San Francisco, CA).

Results

Macrophage Syk and PI3K gamma drive tumor growth and metastasis

Macrophages play an important role in promoting tumor growth and in establishing an immunosuppressive microenvironment that dampens effective T cell responses in tumors (23). Recently, our laboratory and others reported that PI3Kγ is one of the targets that is a major driver of tumor growth and immune suppression (Figure 1A and B) (6,17,24). Herein, we identify that Syk in MΦs promotes tumor immune suppression. Given our previous reports that MΦ specific Syk kinase functions upstream of Rac2 and downstream of $\alpha_4\beta_1$ integrin receptor (16), we sought to evaluate the role of myeloid Syk in regulating tumor growth. We generated conditional Syk knockout mice ($Syk^{MC\text{-}KO}$) in which Syk expression was controlled by LysM cre recombinase, a myeloid cell-specific promoter. Conditional deletion of Syk as confirmed by immunoblotting of BMDMs clearly demonstrate Syk expression only in wild-type ($Syk^{MC\text{-}WT}$) MΦs and not in $Syk^{MC\text{-}KO}$ MΦs (Figure 1C). Furthermore, our results in Figures 1C and D, show that Syk kinase is expressed only in BMDMs, CD11b+ F4/80+ tumor associated MΦs (TAMs), CD19+ B cells and minimally in CD90.2+ T cells, with no expression of Syk in the murine syngeneic tumor cells used in these experiments. To investigate the functional role of MΦ Syk kinase in tumor growth, we used 2 different syngeneic tumors which included: Lewis lung carcinoma (LLC), and B16 melanoma. Tumor growth was reproducibly significantly reduced in $Syk^{MC\text{-}KO}$ animals compared to $Syk^{MC\text{-}WT}$ animals (Figure 1E). Most notably, intravenous injection of B16 tumor cells resulted in significantly reduced lung tumor metastasis in $Syk^{MC\text{-}KO}$ (Figure 1F) and p110γ−/− animals reported earlier by our lab (17).

In order to evaluate the immunological changes in the LLC tumors, CD45+ hematopoietic cells were profiled from $Syk^{MC\text{-}WT}$ and $Syk^{MC\text{-}KO}$ mice using mass cytometry (Cytometry by Time of Flight, CyTOF). Analysis of the total CD45+ leukocytes using Phenograph

clustering (25) revealed 18 different clusters (Figures 1G–H, S1). Among those clusters, we found slight expansion of CD4+ (cluster C18), CD8+ (cluster C13) T cells in $Syk^{MC\text{-}KO}$ tumors with no change in B cell population (cluster C17). Among myeloid cell population, we observed no changes in the CD11b+F4/80+ MΦs (cluster C2), or CD11b +F4/80+CD80+CD86+CX3CR1+CD64+ tissue resident MΦs (Cluster C16) or CD11b+ CD86+CD11c+MHCII+ or CD11c+MHCII+ dendritic cells (cluster C9, C15) (Figure 1H). Interestingly, we found slight expansion in CD11b+Ly6C+ classical monocytes (cluster C6), CD11b+F4/80+CD80+CD86+MHCII+ immunostimulatory MΦ population (cluster C5) in $Syk^{MC\text{-}KO}$ tumors by comparison with decrease in immunosuppressive MΦs, CD11b +$F4/80^{hi}$CD206+TGFb+CD64+ (cluster C11) and myeloid derived suppressor cells or neutrophils, CD11b+LY6C+Ly6G+ (Cluster C8 and C14). Although, the changes in different myeloid populations in $Syk^{MC\text{-}WT}$ and $Syk^{MC\text{-}KO}$ tumors didn't reach to any statistical significance but it provides the evidence that deletion of myeloid Syk showed shifting of immunosuppressive macrophage polarization towards immunostimulatory macrophage population in $Syk^{MC\text{-}KO}$ tumors which might lead to inhibition of tumor growth and metastasis observed in these KO mice.

Syk kinase promotes macrophage polarization and immune suppression

We next investigated whether Syk deletion in MΦs alters expression of genes associated with immune suppression and tumor progression. The expression of genes which mediates immunosuppression in TME (6,18) were significantly higher in TAMs isolated from LLC tumors grown in $Syk^{MC\text{-}WT}$ animals compared to that of $Syk^{MC\text{-}KO}$ animals (Figure 2A). In contrast, expression of immunostimulatory genes (6,18) were significantly enhanced in the TAMs from $Syk^{MC\text{-}KO}$ animals compared to that of $Syk^{MC\text{-}WT}$ tumors (Figure 2A). Moreover, increased arginase activity ($p < 0.01$) and decreased nitrite production (NOS) ($p < 0.001$) was observed in TAMs isolated from $Syk^{MC\text{-}WT}$ LLC tumors compared to those isolated from $Syk^{MC\text{-}KO}$ LLC tumors (Figure 2B). RNA-seq data on LLC TAMs suggest that the expression of genes which mediate immunosuppression in TME, e.g., *Vegf*, *Tgfb*, *Ido2*, *Myc*, *Ccl8*, *Ccl28* are expressed high in $Syk^{MC\text{-}WT}$ and on the contrary, genes involved in antigen presentation and innate immunity are expressed high in $Syk^{MC\text{-}KO}$ (Figure 2C). Interestingly, deletion of Syk did not affect the infiltration of TAMs in the LLC tumors (Cluster C2, Figure 1H), but it increased the expression of major histocompatibility complex (MHC) class II (Figure 2D) and immunostimulatory cytokines and decreased the expression of immunosuppressive genes in TAMs (Figures 2A & C) suggesting that Syk regulates immune suppression.

To determine whether Syk kinase controls transcriptional changes in MΦs, we tested the effect of Syk deletion on lipopolysaccharide (LPS) polarized and IL4 polarized bone marrow derived macrophages (BMDMs). It is well documented that LPS induce MΦ expression of T_H1 cytokines, whereas IL4 signaling stimulates T_H2 response (26). Genes associated with immune stimulation were upregulated in LPS or IL4 stimulated $Syk^{MC\text{-}KO}$ MΦs, while genes associated with immune suppression were downregulated in these MΦs (Figures S2 A–D). Taken together, these results confirm that Syk plays a major role in promoting the immunosuppressive MΦ epigenetic/transcriptional program.

To investigate the mechanism by which Syk regulates macrophage immune responses, ATAC seq was performed. In the IL4 exposed group, most significant immune-related motifs (AP-1, AR, C/EBPB, EGR1, EGR2, HIF2A) were found to be highly enriched in $Syk^{MC\text{-}WT}$ MΦs (Figure 2E). Conversely in the LPS group, the significantly enriched motifs (AP-1, and NF-κB) were mostly found in the $Syk^{MC\text{-}KO}$ MΦs. Existing literature suggests that NF-κB promotes expression of pro-inflammatory cytokines while HIF1α and HIF2α are the transcription factors involved in immunosuppressive MΦ differentiation and suppression of T cell function (27–30). Hence, we determined if genetic deletion of Syk affects the phosphorylation of p65 RelA or stability of hypoxic HIF1α or HIF2α. In consistent with ATAC-seq results we found that deletion of Syk kinase stimulated and sustained p65 RelA phosphorylation, and destabilized hypoxic HIF1α and HIF2α (Figures 2F–G). Together, these results suggest that in addition to PI3Kγ (6), Syk is another molecular switch in TAMs which regulates immune suppression or immune activation.

Syk kinase inhibits CD8+ T cell recruitment and activation

To investigate if the deletion of macrophage Syk promotes the adaptive immune response, we evaluated the recruitment and activation of CD8+ T cells which play an important role in anti-tumor immune responses. Flow cytometric analysis of LLC tumors demonstrate that recruitment of total CD8+ T cells increased in $Syk^{MC\text{-}KO}$ tumors (Figures 3A & B), without significantly altering T cell recruitment in the spleen (Figures S3 A & B). To validate that macrophage Syk inhibits adaptive immune responses, TAMs isolated from $Syk^{MC\text{-}WT}$ and $Syk^{MC\text{-}KO}$ were mixed in 1:1 ratio with LLC tumor cells and were adoptively transferred into different $Syk^{MC\text{-}WT}$ and $Syk^{MC\text{-}KO}$ mice (Figure S3C). WT MΦs adoptively transferred into $Syk^{MC\text{-}WT}$ and $Syk^{MC\text{-}KO}$ mice showed increase in tumor growth, while adoptive transfer of KO MΦs suppressed tumor growth in $Syk^{MC\text{-}WT}$ and $Syk^{MC\text{-}KO}$ mice (Figure 3C). In addition, Syk inhibition did not reduce tumor growth in CD8-depleted mice suggesting that Syk inhibition reduces tumor growth by recruiting and activating CD8+ T cells (Figure 3D). Moreover, we found that CD90+ T cells isolated from $Syk^{MC\text{-}KO}$ LLC tumors expressed significantly more *Ifng and Gzmb* as compared to that from WT tumors (Figure 3E) suggesting that deletion of Syk kinase activates T cell-mediated anti-tumor immune response *in vivo*. RNA-seq analysis performed on LLC tumors implanted in $Syk^{MC\text{-}KO}$ tumors showed an increase in *Prf, Gzm, Klre1* and several other genes which are involved in activation of cytotoxic T cells (Figure 3F). We did not observe any difference in the proliferative capacity of T cells between $Syk^{MC\text{-}WT}$ and $Syk^{MC\text{-}KO}$ animals (Figure S4D). Taken together, our results demonstrate that Syk kinase inhibition in MΦs indirectly promotes cytotoxic adaptive immune responses in the tumor.

Pharmacological inhibition of Syk kinase blocks tumor growth, immunosuppression and increases CD8+ T cell activation

Given that the conditional deletion of Syk kinase inhibits tumor growth and intratumoral immunosuppression, we speculated that pharmacological inhibitors of Syk could similarly inhibit tumor growth and induce an anti-tumor response. To test this, we used commercially available specific Syk kinase inhibitor, Fostamatinib (R788) (31). Tumor growth and metastasis were significantly suppressed in the mice treated with Syk inhibitor compared to vehicle treated tumors (Figure 4A). Importantly, R788 had no effect on viability of LLC

cells (Figure S4). Pharmacological blockade of Syk kinase significantly inhibited expression of immunosuppressive genes and increased expression of immunostimulatory genes in TAMs purified from LLC tumors (Figure 4B). Moreover, R788-treated LLC tumors showed increased infiltration of CD8+ T cells with no significant reduction in number of regulatory T cells (Figure 4D). Interestingly, we observed increased $CD44^{hi}CD62L^{lo}$ effector T cells (gated on CD8+T cells) and cytotoxic T cells in R788 treated tumors (Figures 4E & F), and these findings are not due to differences in T-cell proliferation as we observed no effect of R788 on T cell proliferation *ex vivo* (Figure S5A).

To determine whether Syk suppresses anti-tumor adaptive immune response *in vivo*, we injected B16-OVA cells in C57BL/6 mice and characterized OVA-specific CD8+ T cells, in R788 treated tumors. Using $H\text{-}2K^{b}$ tetramers containing the OVA protein-derived peptide SIINFEKL, we found that R788 treatment significantly blocked tumor growth and increased OVA specific CD8+ T cells in the tumor draining lymph nodes (Figures S5 B & C). These results provide evidence that Syk kinase suppress the antigen-specific adaptive immune response in the TME *in vivo.*

To explore the possibility that Syk inhibitors might synergize with T cell check point inhibitors, we determined the effect of R788 in combination with anti-PDL1 in B16 melanoma cells. Both anti-PDL1 and R788 substantially inhibited B16-OVA tumor growth. While the combination of R788 and anti-PDL1 showed no significant additive effect on Syk inhibition (Figure S5B) in resistant B16 model, but $CD44^{hi}$ and $CD62L^{lo}$ effector T cells were significantly increased in the combination treated group compared to monotherapy treated groups (Figures S5C–E). Although, the combination of R788 and anti-PDL1 didn't work well in B16 model, further *in vivo* synergistic studies are ongoing in our lab to explore the efficacy of this combination regimen in other cancer models. Taken together, these results validate Syk as an immuno-oncology drug candidate with equivalent *in vivo* activity compared anti-PDL1 blockade in this immune competent model.

Syk and PI3Kγ two molecular targets in TAMs: In silico design of SRX3207, a novel dual Syk/PI3K inhibitory chemotype

The concept of combinatorial therapeutics recently emerged as effective strategy to synergistically activate antitumor immunity (18,32–34). Our lab has developed a drug discovery paradigm that uses computational methods to engineer a single chemotype to inhibit two separate targets in one small molecule and demonstrated proof of concept for greater antitumor efficacy *in vivo* (18,34). Herein, we apply this technology to two immuno-oncology targets, PI3K (6) and Syk kinase (data presented in this manuscript).

We utilized multiple X-ray crystallographic datasets in the form of PDB files of Syk, ZAP70, PI3K/p110α and PI3K/p110γ (PDB 4XG9, 1U59, 4JPS and 4XZ4, respectively) to engineer a small molecule chemotype which will contain two distinct "warheads" within the thienopyranone scaffold (35) to bind to the ATP binding pockets of PI3K isoforms and Syk kinase. Figure 5A shows the docking of SRX3188 in Syk active site which showed that this inhibitor is engaged via hydrogen-bond interactions with the amide and carbonyl groups of Ala451, the sulfur atom of methionine Met450, and the hydroxyl group and Arg498, while the azetidine nitrogen is making a charge interaction with the carboxylate group of Asp512

in the same way the co-crystallized inhibitor in 4XG9 is observed, confirming the expected binding mode and necessary hydrogen-bond interactions. When modeling SRX3188 in ZAP70 it was observed that, contrary to staurosporine which in the crystal structure of ZAP70 is found to make 2 key hydrogen bond interactions with Glu415 and Ala417, SRX3188 does not manifest this interaction predicting no affinity towards ZAP70, a tyrosine kinase homologous to Syk.

Modeling of SRX3188 in PI3K/p110α indicates that the TP core of SRX3188 binds as expected establishing a hydrogen bond interaction between the morpholine group and Val815, the pyrazole ring forming a π-π T-shaped interaction with Trp780, and the azetidine nitrogen is making a charge interaction with the carboxylate group of Glu798 (Figure 5B). Modeling of SRX3188 in PI3K/p110γ also showed an expected hydrogen bond interaction between the morpholine group and Val882, and the predicted π-π T-shaped interaction of the pyrazole ring with Trp812 also observed with PI3K/p110α (Figure 5C). It was also predicted the hydroxyl group of the azetidine group occupies a region where no additional interactions are engaged with this kinase.

Since the proximity of the hydroxyl group of the azetidine group to the Syk's backbone and the non-favorable electrostatic microenvironment surrounding the hydroxyl group were a concern, the hydroxyl group was removed leading to the design and synthesis of SRX3207. *In silico* docking studies of SRX3207 against Syk indicated this analog would bind to Syk in the same way as SRX3188 does. Similarly, docking results of SRX3207 against PI3K/p110α and PI3K/p110γ indicate similar binding modes while exhibiting no affinity towards ZAP70. The final chemotype designed was synthesized and tested in cell free systems for potency against Syk, ZAP70 and PI3K isoforms p110α, p110β, p110γ and p110δ (Figure 5D). The first generation chemotype, SRX3188 had excellent Syk inhibitory activity (IC_{50} of 20 nM) but poor PI3K inhibitory potency. Extensive modeling of the p110α and p110γ crystal structures (PDB 4JPS and PDB 4XZ4, respectively) enabled a structure activity relation analysis (SAR) to develop the second-generation prototype inhibitor, SRX3207 with potent Syk (30 nM) and acceptable PI3K inhibitory properties *in vitro*. Figure 5D shows the chemical structure of SRX3188 and SRX3207.

Pharmacokinetic and pharmacodynamics properties of SRX3207

Results in Figure 5E shows that SRX3207 is a dual Syk kinase/PI3K inhibitor which hits both targets in the same molecule at nM potency with minimal off-target effects (Figure 5E, Supplementary Table S1). Figure S6A shows that both SRX3188 and SRX3207 potently blocks phosphorylation of Syk at 348 site and Y525/526 site which are required for complete activation of Syk, described in detail in next section. Moreover, SRX3207, is able to block p-AKT at 10 μM conc. (Figure S6A). Finally, we profiled SRX3207 against a library of 468 known kinases which demonstrated a selectivity index (SI) of 0.079 (Figure S6B) documenting a high level selectivity of this *in silico* engineered dual inhibitory compound. SRX3207 has selectivity score of 8 which is defined as number of kinases hit by the molecule with scores less than 1 [S (1)] (36). Because of both the high potency and excellent kinase selectivity of SRX3207 an oral prototype formulation of SRX3207 was prepared using Pharmatek's Hot Rod formulations to be used in preliminary *in vivo* studies.

Preliminary PK studies in mice via both the i.v. and oral route indicated a half-life of about 5 hours but with a low bioavailability of only around 2% (Figures 5 F & G). Despite this being a non-optimized formulation the oral administration of this prototype formulation of SRX3207 yielded significant anti-tumor activity (Figure 6). Additional ADME studies indicate SRX3207 has sufficient solubility in water (43 μM) relative to its target potencies but suffers from a metabolic liability with a CLint (μL/min/mg protein) of 74. Further studies are in progress to optimize the prototype SRX3207 molecule from an ADME standpoint while preserving the desired potencies on the Syk and PI3K target enzymes. In the meantime, the proof of concept benefits from having a single molecule with both Syk and PI3K inhibition properties are illustrated with the prototype molecule SRX3207.

SRX3207 blocks tumor immunosuppression and increases anti-tumor immunity

We next determined if SRX3207 blocks immune suppressive MΦ polarization. Interestingly, we found that SRX3207 potently blocks immunosuppressive gene expression effectively at very low dose compared to commercially available p110γ inhibitor (IPI-549) or Syk inhibitor (R488) alone (Figures S6 C & D). Moreover, SRX3207 at 10 mg/kg dose blocked tumor growth and increased survival effectively as compared to IPI549 and R788 treated groups at similar doses without toxicity (Figures 6A and B & S7A). Furthermore it reduced immunosuppressive MΦ polarization and increased infiltration and cytotoxicity of CD8+ T cells in LLC tumors and increased expression of *Ifng* and *Gzmb* in 3207 treated LLC tumors (Figures 6C–E & S7B). Most notably, SRX3207 didn't affect T cell proliferation (Fig. S7C). Moreover, administration of SRX3207 didn't block CT26 tumor growth in NSG mice but blocked tumor growth in Balb/c mice suggesting that SRX3207 blocks tumor growth due to its effect on immune compartment (Fig. S7 D–E). Moreover, depleting MΦs with anti-CSF1R (CD115) antibody treatment alone significantly blocked LLC tumor growth, but the combination with R788 or SRX3207 had no additive effects (Figure S7F). Taken together, these results validate the efficacy of this novel dual Syk/PI3K inhibitor in blocking immune suppression and activating the adaptive immune response and opened new opportunities to explore it in combination with check point inhibitors.

$\alpha_4\beta_1$-Syk-p110γ axis in macrophages controls HIF1α stability under hypoxia, immunosuppression and tumor immunity

In MΦs, Syk kinase is known to be activated upon binding to phosphorylated ITAMs of Fc gamma receptor, or by binding to the cytoplasmic domains of integrin adhesion receptors, most notably β_1 and β_3 integrin (9). Our results in Fig. S8A shows that only $\alpha_4\beta_1$ integrin can maximally activate Syk at Y348 site in MΦs isolated from the TME (Figure S8A), and BMDMs isolated from α_4Y991A mice are defective in phosphorylating Syk at Y348 site (Figure S8B). These results suggest that Syk is phosphorylated downstream of $\alpha_4\beta_1$ integrin and mediates tumor growth and immunosuppression. Interestingly, Figure 6F illustrates that administration of R788 didn't show additive reduction in tumor growth in $Syk^{MC\text{-}KO}$ mice, while IPI549 or SRX3207 significantly decreased tumor growth in the $Syk^{MC\text{-}KO}$ mice. These results suggest that Syk and p110γ are two separate molecular entities which promote tumor growth and their simultaneous inhibition with single molecule is good strategy to reduce tumor growth and immunosuppression. Our published results (17) and data presented here have shown that genetic or pharmacological deletion of p110γ and/or Syk results in

hypoxic degradation of HIF1/2α and this effect is completely blocked by MG132, a proteasome inhibitor (Figure S8C). Figure 6G shows the schematic of Syk and p110γ regulation on tumor immunosuppression.

DISCUSSION

TAMs are reported as the most abundant immune cells in the TME of solid tumors, where they release immunosuppressive factors that inhibit T cell-mediated anti-tumor immune response (37). Therapeutic approaches that are aimed at blocking tumor immunosuppression by inhibiting macrophage polarization have shown great efficacy in murine cancer models (38,39) and open new and effective strategies to treat cancer.

In this report, we focused on two major immuno-oncology targets, namely Syk kinase (reported in this manuscript) and PI3Kγ (6,17). We provided several lines of evidence to prove that inhibition of Syk kinase is associated with reduction of tumor growth, macrophage mediated immunosuppression and activation of adaptive immune responses in TME (Figures 1–4). Although recent study has shown the efficacy of Syk inhibitor in solid tumors (40) but the role of MΦs in activating adaptive immune responses has never been reported. Our results have shown that Syk kinase is minimally expressed in T cells and inhibition of this kinase increases infiltration and activation of CD8+ T cells with reduction in percentage of CD4+T cells, which can be explained by reduction in the number of immunosuppressive CD4+ regulatory T cells (Treg). Our initial preliminary results have shown decrease in number of Tregs in R788 treated tumors but the results didn't reach to significance (Fig. 4D). Recent studies have shown that similar to dendritic cells, macrophages can also prime CD8+ T cells to generate cytotoxic effector cells *in vivo* (41). Our results in Figures 2 and 3 clearly provide evidence that Syk kinase inhibition in MΦs indirectly promotes cytotoxic adaptive immune responses and represents a major immune-oncology target.

Herein, we describe the *in silico* design and synthesis of a novel dual Syk-PI3K inhibitor, SRX3207 which potently inhibited Syk and PI3K signaling and augmented the anti-tumor immune response in lung carcinoma tumor model with no toxicity (Figure 6). Taken in context (16,17,42) the results presented here elucidate the mechanistic interconnection of integrin $\alpha_4\beta_1$, p110γ, Syk, HIF axis in MΦs. In addition, data provided in Figure 6F, provides the rationale to target both Syk and p110γ with single molecule for effective anti-tumor immunity and to explore SRX3207 in combination with checkpoint inhibitors in cancers driven by MΦ mediated immunosuppression.

Supplementary Material

Refer to Web version on PubMed Central for supplementary material.

Acknowledgements:

This work was supported by R01 CA215651 to Donald L. Durden.

Abbreviations.

MΦ	macrophage
TME	tumor microenvironment
TAM	tumor associated macrophages
TGF	beta transforming growth factor
VEGF	vascular endothelial growth factor
BMDM	bone marrow derived macrophages grown in MCSF
MCSF	macrophage colony stimulating factor
ECM	extracellular matrix
MMP	matrix metalloproteinase

References:

1. Chanmee T, Ontong P, Konno K, Itano N. Tumor-associated macrophages as major players in the tumor microenvironment. Cancers (Basel) 2014;6(3):1670–90 doi 10.3390/cancers6031670 cancers6031670 [pii]. [PubMed: 25125485]
2. Mantovani A, Sica A. Macrophages, innate immunity and cancer: balance, tolerance, and diversity. Curr Opin Immunol 2010;22(2):231–7 doi 10.1016/j.coi.2010.01.009S0952-7915(10)00010-5 [pii]. [PubMed: 20144856]
3. Pollard JW. Tumour-educated macrophages promote tumour progression and metastasis. Nat Rev Cancer 2004;4(1):71–8 doi 10.1038/nrc1256 nrc1256 [pii]. [PubMed: 14708027]
4. Hagemann T, Lawrence T, McNeish I, Charles KA, Kulbe H, Thompson RG, et al. "Re-educating" tumor-associated macrophages by targeting NF-kappaB. J Exp Med 2008;205(6):1261–8 doi 10.1084/jem.20080108 jem.20080108 [pii]. [PubMed: 18490490]
5. Pello OM, De Pizzol M, Mirolo M, Soucek L, Zammataro L, Amabile A, et al. Role of c-MYC in alternative activation of human macrophages and tumor-associated macrophage biology. Blood 2012;119(2):411–21 doi 10.1182/blood-2011-02-339911 blood-2011-02-339911 [pii]. [PubMed: 22067385]
6. Kaneda MM, Messer KS, Ralainirina N, Li H, Leem CJ, Gorjestani S, et al. PI3Kgamma is a molecular switch that controls immune suppression. Nature 2016;539(7629):437–42 doi 10.1038/nature19834 nature19834 [pii]. [PubMed: 27642729]
7. Berton G, Mocsai A, Lowell CA. Src and Syk kinases: key regulators of phagocytic cell activation. Trends Immunol 2005;26(4):208–14 doi S1471-4906(05)00026-8 [pii] 10.1016/j.it.2005.02.002. [PubMed: 15797511]
8. Pradip D, Peng X, Durden DL. Rac2 specificity in macrophage integrin signaling: potential role for Syk kinase. J Biol Chem 2003;278(43):41661–9 doi 10.1074/jbc.M306491200 M306491200 [pii]. [PubMed: 12917394]
9. Mocsai A, Ruland J, Tybulewicz VL. The SYK tyrosine kinase: a crucial player in diverse biological functions. Nat Rev Immunol 2010;10(6):387–402 doi 10.1038/nri2765 nri2765 [pii]. [PubMed: 20467426]
10. Ghotra VP, He S, van der Horst G, Nijhoff S, de Bont H, Lekkerkerker A, et al. SYK is a candidate kinase target for the treatment of advanced prostate cancer. Cancer Res 2015;75(1):230–40 doi 10.1158/0008-5472.CAN-14-06290008-5472.CAN-14-0629 [pii]. [PubMed: 25388286]
11. Yu Y, Suryo Rahmanto Y, Lee MH, Wu PH, Phillip JM, Huang CH, et al. Inhibition of ovarian tumor cell invasiveness by targeting SYK in the tyrosine kinase signaling pathway. Oncogene

2018;37(28):3778–89 doi 10.1038/s41388-018-0241-010.1038/s41388-018-0241-010.1038/s41388-018-0241-010.1038/s41388-018-0241-0 [pii]. [PubMed: 29643476]

12. Layton T, Stalens C, Gunderson F, Goodison S, Silletti S. Syk tyrosine kinase acts as a pancreatic adenocarcinoma tumor suppressor by regulating cellular growth and invasion. Am J Pathol 2009;175(6):2625–36 doi 10.2353/ajpath.2009.090543 S0002-9440(10)60770-5 [pii]. [PubMed: 19893036]
13. Bailet O, Fenouille N, Abbe P, Robert G, Rocchi S, Gonthier N, et al. Spleen tyrosine kinase functions as a tumor suppressor in melanoma cells by inducing senescence-like growth arrest. Cancer Res 2009;69(7):2748–56 doi 10.1158/0008-5472.CAN-08-26900008-5472.CAN-08-2690 [pii]. [PubMed: 19293188]
14. Yi YS, Son YJ, Ryou C, Sung GH, Kim JH, Cho JY. Functional roles of Syk in macrophage-mediated inflammatory responses. Mediators Inflamm 2014;2014:270302 doi 10.1155/2014/270302. [PubMed: 25045209]
15. De P, Peng Q, Traktuev DO, Li W, Yoder MC, March KL, et al. Expression of RAC2 in endothelial cells is required for the postnatal neovascular response. Exp Cell Res 2009;315(2):248–63. [PubMed: 19123268]
16. Joshi S, Singh AR, Zulcic M, Bao L, Messer K, Ideker T, et al. Rac2 controls tumor growth, metastasis and M1-M2 macrophage differentiation in vivo. PLoS One 2014;9(4):e95893 doi 10.1371/journal.pone.0095893PONE-D-13-51894 [pii]. [PubMed: 24770346]
17. Joshi S, Singh AR, Zulcic M, Durden DL. A macrophage-dominant PI3K isoform controls hypoxia-induced HIF1alpha and HIF2alpha stability and tumor growth, angiogenesis, and metastasis. Mol Cancer Res 2014;12(10):1520–31 doi 10.1158/1541-7786.MCR-13-06821541-7786.MCR-13-0682 [pii]. [PubMed: 25103499]
18. Joshi S, Singh AR, Liu KX, Pham TV, Zulcic M, Skola D, et al. SF2523: Dual PI3K/BRD4 inhibitor blocks tumor immunosuppression and promotes adaptive immune responses in cancer. Mol Cancer Ther 2019 doi molcanther.1206.2018 [pii]10.1158/1535-7163.MCT-18-1206 1535-7163.MCT-18-1206 [pii].
19. Park H, Cox D. Syk regulates multiple signaling pathways leading to CX3CL1 chemotaxis in macrophages. J Biol Chem 2011;286(17):14762–9 doi 10.1074/jbc.M110.185181 M110.185181 [pii]. [PubMed: 21388954]
20. Beitz LO, Fruman DA, Kurosaki T, Cantley LC, Scharenberg AM. SYK is upstream of phosphoinositide 3-kinase in B cell receptor signaling. J Biol Chem 1999;274(46):32662–6. [PubMed: 10551821]
21. Feral CC, Rose DM, Han J, Fox N, Silverman GJ, Kaushansky K, et al. Blocking the alpha 4 integrin-paxillin interaction selectively impairs mononuclear leukocyte recruitment to an inflammatory site. J Clin Invest 2006;116(3):715–23 doi 10.1172/JCI26091. [PubMed: 16470243]
22. Guillermo A Morales JRG, Donald L. Durden; Thienopyranones and furanopyranones as checkpoint inhibitors and modulators of anti-tumor immunity patent Patent WO2018226739A1 (PCT/US2018/036122). 2018.
23. Sica A, Mantovani A. Macrophage plasticity and polarization: in vivo veritas. J Clin Invest 2012;122(3):787–95 doi 10.1172/JCI5964359643 [pii]. [PubMed: 22378047]
24. De Henau O, Rausch M, Winkler D, Campesato LF, Liu C, Cymerman DH, et al. Overcoming resistance to checkpoint blockade therapy by targeting PI3Kgamma in myeloid cells. Nature 2016;539(7629):443–7 doi 10.1038/nature20554nature20554nature20554 [pii]. [PubMed: 27828943]
25. Chen H, Lau MC, Wong MT, Newell EW, Poidinger M, Chen J. Cytofkit: A Bioconductor Package for an Integrated Mass Cytometry Data Analysis Pipeline. PLoS Comput Biol 2016;12(9):e1005112 doi 10.1371/journal.pcbi.1005112PCOMPBIOL-D-16-00603 [pii]. [PubMed: 27662185]
26. Martinez FO, Gordon S. The M1 and M2 paradigm of macrophage activation: time for reassessment. F1000Prime Rep 2014;6:13 doi 10.12703/P6-1313 [pii]. [PubMed: 24669294]
27. Leblond MM, Gerault AN, Corroyer-Dulmont A, MacKenzie ET, Petit E, Bernaudin M, et al. Hypoxia induces macrophage polarization and re-education toward an M2 phenotype in U87 and

U251 glioblastoma models. Oncoimmunology 2016;5(1):e1056442 doi 10.1080/2162402X.2015.10564421056442 [pii]. [PubMed: 26942063]

28. Takeda N, O'Dea EL, Doedens A, Kim JW, Weidemann A, Stockmann C, et al. Differential activation and antagonistic function of HIF-{alpha} isoforms in macrophages are essential for NO homeostasis. Genes Dev 2010;24(5):491–501 doi 10.1101/gad.188141024/5/491 [pii]. [PubMed: 20194441]
29. Westendorf AM, Skibbe K, Adamczyk A, Buer J, Geffers R, Hansen W, et al. Hypoxia Enhances Immunosuppression by Inhibiting CD4+ Effector T Cell Function and Promoting Treg Activity. Cell Physiol Biochem 2017;41(4):1271–84 doi 10.1159/000464429000464429 [pii]. [PubMed: 28278498]
30. Doedens AL, Stockmann C, Rubinstein MP, Liao D, Zhang N, DeNardo DG, et al. Macrophage expression of hypoxia-inducible factor-1 alpha suppresses T-cell function and promotes tumor progression. Cancer Res 2010;70(19):7465–75 doi 10.1158/0008-5472.CAN-10-14390008-5472.CAN-10-1439 [pii]. [PubMed: 20841473]
31. Yamamoto N, Takeshita K, Shichijo M, Kokubo T, Sato M, Nakashima K, et al. The orally available spleen tyrosine kinase inhibitor 2-[7-(3,4-dimethoxyphenyl)-imidazo[1,2-c]pyrimidin-5-ylamino]nicotinamide dihydrochloride (BAY 61–3606) blocks antigen-induced airway inflammation in rodents. J Pharmacol Exp Ther 2003;306(3):1174–81 doi 10.1124/jpet.103.052316jpet.103.052316 [pii]. [PubMed: 12766258]
32. Bayat Mokhtari R, Homayouni TS, Baluch N, Morgatskaya E, Kumar S, Das B, et al. Combination therapy in combating cancer. Oncotarget 2017;8(23):38022–43 doi 10.18632/oncotarget.1672316723 [pii]. [PubMed: 28410237]
33. Joshi S, Durden DL. Combinatorial Approach to Improve Cancer Immunotherapy: Rational Drug Design Strategy to Simultaneously Hit Multiple Targets to Kill Tumor Cells and to Activate the Immune System. J Oncol 2019;2019:5245034 doi 10.1155/2019/5245034. [PubMed: 30853982]
34. Andrews FH, Singh AR, Joshi S, Smith CA, Morales GA, Garlich JR, et al. Dual-activity PI3K-BRD4 inhibitor for the orthogonal inhibition of MYC to block tumor growth and metastasis. Proc Natl Acad Sci U S A 2017;114(7):E1072–E80 doi 10.1073/pnas.1613091114161309111413091114 [pii]. [PubMed: 28137841]
35. Morales GA, Garlich JR, Su J, Peng X, Newblom J, Weber K, et al. Synthesis and cancer stem cell-based activity of substituted 5-morpholino-7H-thieno[3,2-b]pyran-7-ones designed as next generation PI3K inhibitors. J Med Chem 2013;56(5):1922–39 doi 10.1021/jm301522m. [PubMed: 23410005]
36. Miduturu CV, Deng X, Kwiatkowski N, Yang W, Brault L, Filippakopoulos P, et al. High-throughput kinase profiling: a more efficient approach toward the discovery of new kinase inhibitors. Chem Biol 2011;18(7):868–79 doi 10.1016/j.chembiol.2011.05.010S1074-5521(11)00201-8 [pii]. [PubMed: 21802008]
37. Gabrilovich DI, Nagaraj S. Myeloid-derived suppressor cells as regulators of the immune system. Nat Rev Immunol 2009;9(3):162–74 doi 10.1038/nri2506nri2506 [pii]. [PubMed: 19197294]
38. Kamran N, Kadiyala P, Saxena M, Candolfi M, Li Y, Moreno-Ayala MA, et al. Immunosuppressive Myeloid Cells' Blockade in the Glioma Microenvironment Enhances the Efficacy of Immune-Stimulatory Gene Therapy. Mol Ther 2017;25(1):232–48 doi S1525-0016(16)45350-5 [pii]10.1016/j.ymthe.2016.10.003. [PubMed: 28129117]
39. Devaud C, John LB, Westwood JA, Darcy PK, Kershaw MH. Immune modulation of the tumor microenvironment for enhancing cancer immunotherapy. Oncoimmunology 2013;2(8):e25961 doi 10.4161/onci.259612013ONCOIMM0165 [pii]. [PubMed: 24083084]
40. Jessica J Sappal MT, Zhongmin Xiang, Stephen Tirrell, Rudy Christmas, Jie Yu, Mengkun Zhang and Karuppiah Kannan. TAK-659, a SYK kinase inhibitor, demonstrates preclinical antitumor activity in solid tumor models. 2018.
41. Broz ML, Binnewies M, Boldajipour B, Nelson AE, Pollack JL, Erle DJ, et al. Dissecting the tumor myeloid compartment reveals rare activating antigen-presenting cells critical for T cell immunity. Cancer Cell 2014;26(5):638–52 doi 10.1016/j.ccell.2014.09.007S1535-6108(14)00370-5 [pii]. [PubMed: 25446897]
42. Joshi S, Singh AR, Durden DL. MDM2 regulates hypoxic hypoxia-inducible factor 1alpha stability in an E3 ligase, proteasome, and PTEN-phosphatidylinositol 3-kinase-AKT-dependent manner. J

Biol Chem 2014;289(33):22785–97 doi 10.1074/jbc.M114.587493M114.587493 [pii]. [PubMed: 24982421]

43. Becht E, McInnes L, Healy J, Dutertre CA, Kwok IWH, Ng LG, et al. Dimensionality reduction for visualizing single-cell data using UMAP. Nat Biotechnol 2018 doi 10.1038/nbt.4314nbt.4314 [pii].

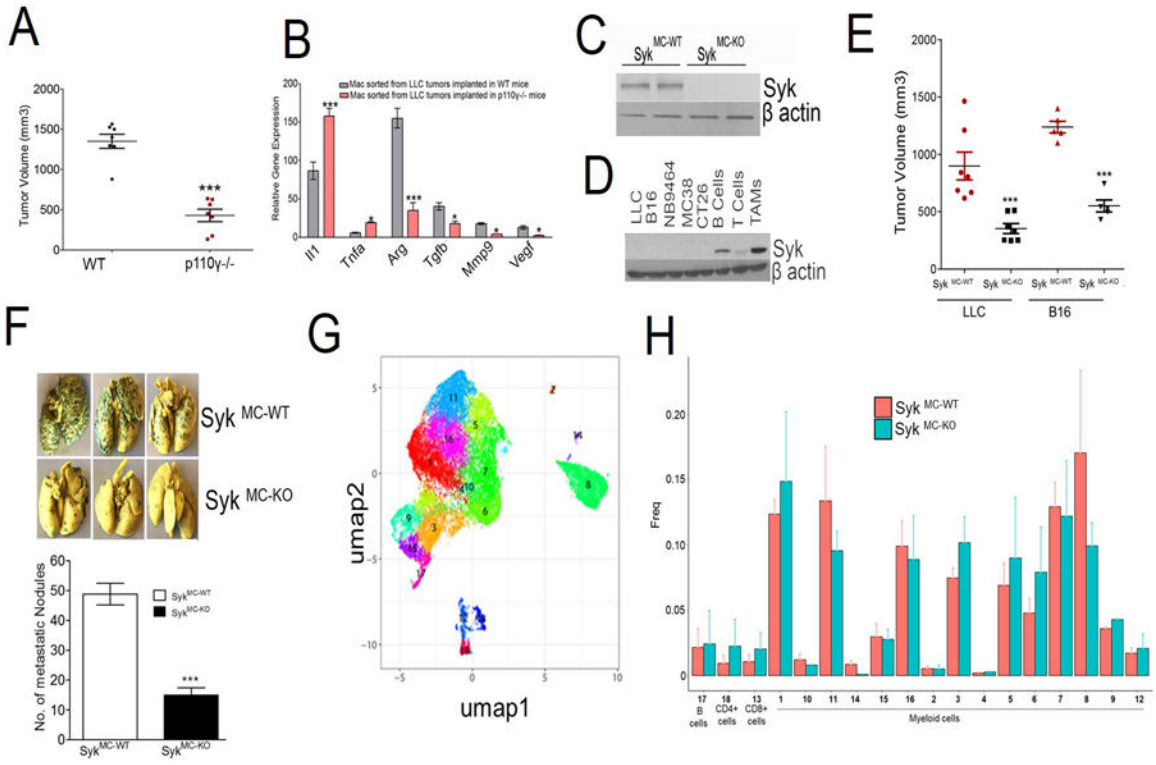

Figure 1: Macrophage Syk and PI3Kγ are required for tumor growth and metastasis.

A. Tumor volume of LLC tumors implanted in WT and p110γ −/− mice (n=7), $p < 0.001$ compared to WT tumors, t test. **B.** mRNA analysis of immunostimulatory or immune suppressive genes in TAMs sorted from tumors from Fig. A. (n= 3), * represents $p < 0.05$, ***represents $p < 0.001$, t test. **C.** Western blot analysis showing deletion of Syk kinase in $Syk^{MC\text{-}KO}$ BMDMs (n = 2). **D.** Western blot of Syk and β actin in cell lines, CD19+ B cells, CD90.2 T cells and CD11b+F4/80+ TAMs. **E.** Tumor volume of LLC, or B16F10 cells implanted in $Syk^{MC\text{-}WT}$ and $Syk^{MC\text{-}KO}$ mice (n = 8–10). *** shows $p < 0.001$ compared to WT tumors, one-way ANOVA using Tukey's multiple comparison tests. **F.** Upper panel shows images of metastasized lungs of $Syk^{MC\text{-}WT}$ and $Syk^{MC\text{-}KO}$ mice (n=3) injected intravenously with B16 melanoma and lower panel shows quantitative analysis of the data (lower panel). **G.** Mass cytometry analysis of CD45+ leukocytes isolated from LLC tumors inoculated in $Syk^{MC\text{-}WT}$ and $Syk^{MC\text{-}KO}$. Figure represents uniform manifold approximation and projection (UMAP, (43) plot of CD45+ leukocytes overlaid with color coded clusters. **H.** Frequency of clusters of different immune cell infiltrates. Data are representative of mean ± SEM (n = 2 mice per group).

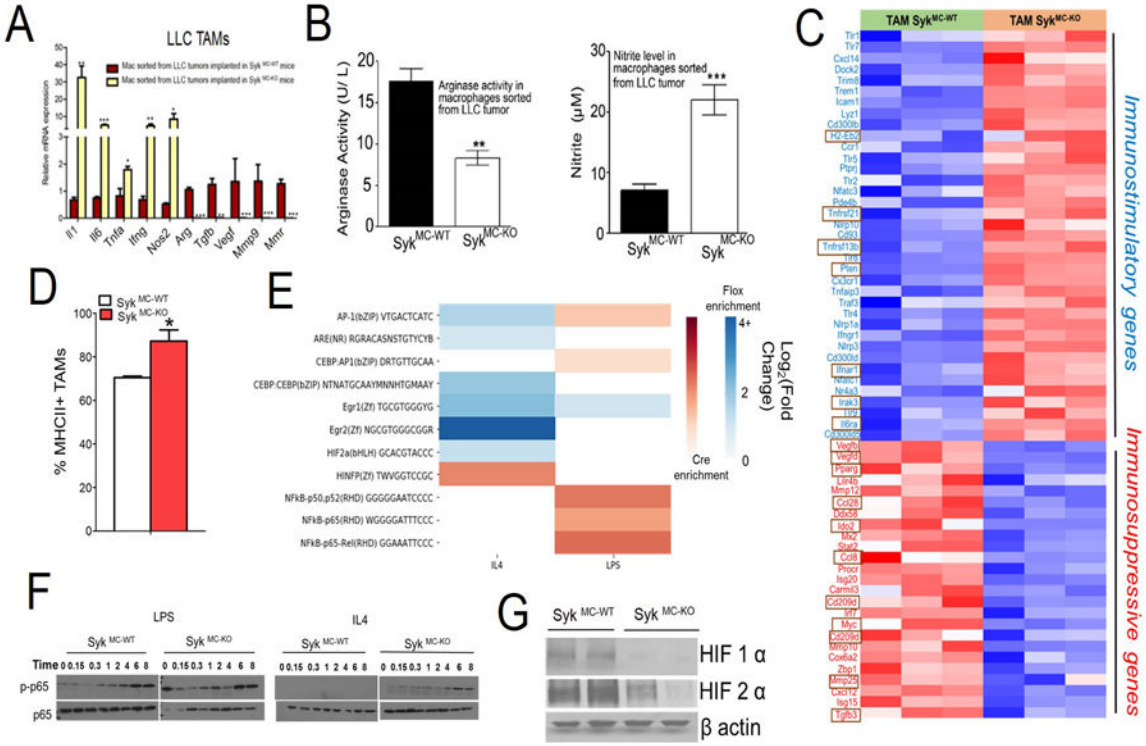

Figure 2: Syk kinase promotes macrophage polarization and immune suppression.

A. RTPCR analysis of cDNAs reflecting TAMs isolated from LLC tumors grown in $Syk^{MC\text{-}WT}$ and $Syk^{MC\text{-}KO}$ animals (n=3), student's t-test. **B.** Arginase (Left panel) and nitrite production (Right panel) was assayed in the TAMs isolated from the tumors (n=3). **C.** Heat map of immune related mRNA expression in $Syk^{MC\text{-}WT}$ versus $Syk^{MC\text{-}KO}$ TAMs isolated from LLC tumors implanted in these mice (n=3). **D.** MHC II expression on $Syk^{MC\text{-}WT}$ and $Syk^{MC\text{-}KO}$ TAMs gated on CD11b+F4/80+ population (n=4)**. E.** Differential enrichment heatmap of Log-2 fold change for immune-related transcription factor binding motifs in open chromatin segments, found via ATAC-seq, of cre and flox macrophages exposed to IL4 and LPS. Blue-colored cells represent higher enrichment in flox ($Syk^{MC\text{-}WT}$) mice and red-colored cells represent higher enrichment in cre ($Syk^{MC\text{-}KO}$) mice. **F.** Immunoblotting of p-p65 (pRelA), p-65 (RelA), in LPS or IL4 stimulated BMDMs from $Syk^{MC\text{-}WT}$ vs $Syk^{MC\text{-}KO}$ mice. **G.** Western blot analysis of nuclear extracts for HIF1α or HIF2α from $Syk^{MC\text{-}WT}$ vs $Syk^{MC\text{-}KO}$ BMDMs incubated under hypoxic conditions (1% O_2). All experiments were performed 2–3 times. Graphs in A, B and D represent mean ± SEM, where * represents $p < 0.05$, ** represents $p < 0.01$, ***represents $p < 0.0001$, analyzed by t test.

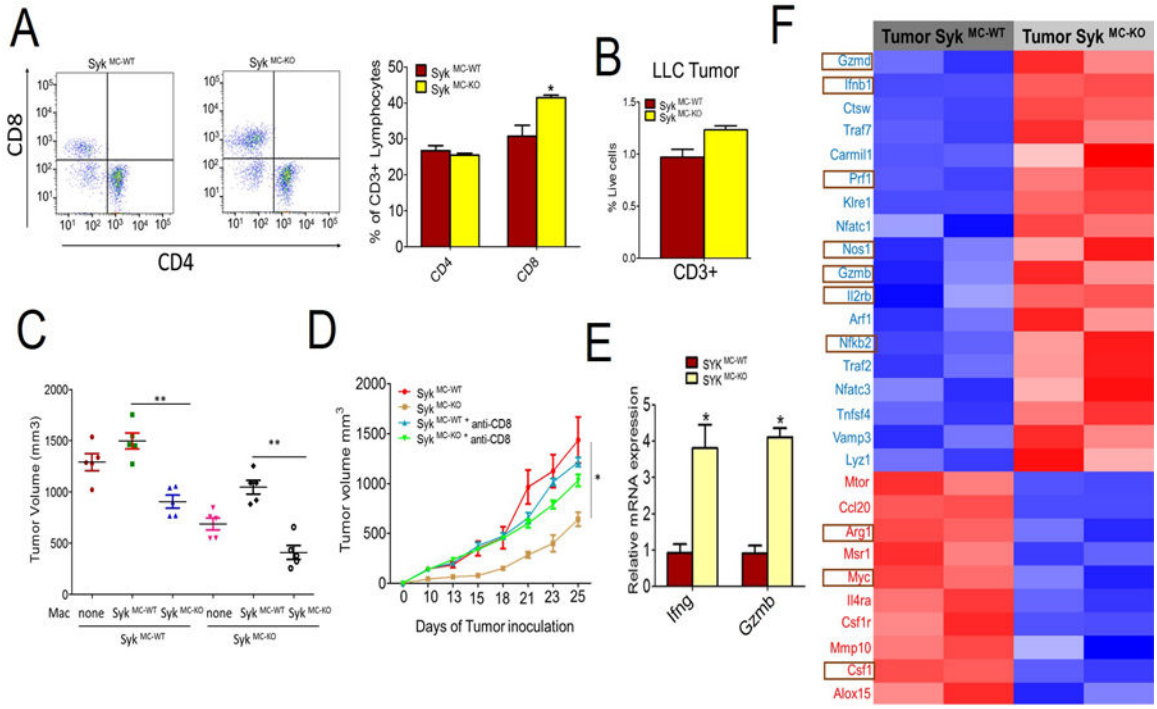

Figure 3: Syk kinase inhibits CD8+ T cell recruitment and activation.

A and B. Flow cytometric representation of percentage of CD4+ and CD8+ T cells (gated on CD3+ cells) (A, left panel) and quantification of these cells (A, right panel) and CD3+ cells (B) in the LLC tumors implanted in Syk$^{MC\text{-}WT}$ and Syk$^{MC\text{-}KO}$ mice. (n=3, p<.05, t test) **C.** Tumor volumes of LLC tumors implanted in Syk$^{MC\text{-}WT}$ and Syk$^{MC\text{-}KO}$ animals adoptively transferred with TAMs from Syk$^{MC\text{-}WT}$ and Syk$^{MC\text{-}KO}$ animals. Data was analyzed by one-way ANOVA using Tukey's multiple comparisons, ** represents $p < 0.01$ compared to Syk$^{MC\text{-}WT}$. **D.** LLC tumor volume from Syk$^{MC\text{-}WT}$ and Syk$^{MC\text{-}KO}$ mice treated with anti-CD8 or isotype control antibodies (n=5). **E.** mRNA expression of Ifng and Gzmb in LLC tumors implanted in Syk$^{MC\text{-}WT}$ and Syk$^{MC\text{-}KO}$ mice (n=5, $p < 0.05$, t test). **F.** Heat map of log2 fold differences from sample wise mean expression for selected T cell activation genes that were differentially expressed in LLC tumors from Syk$^{MC\text{-}WT}$ versus Syk$^{MC\text{-}KO}$ mice conditions (n=2). Graphs in A-E represent mean ± SEM.

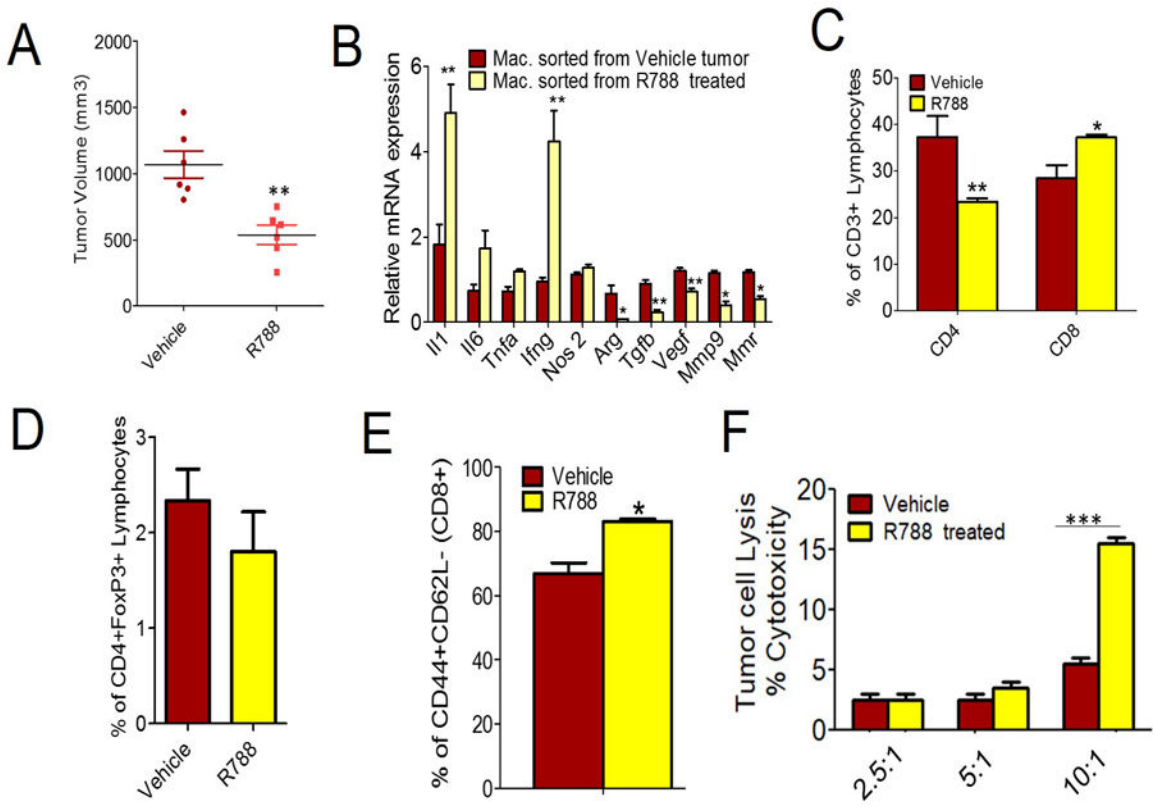

Figure 4: Pharmacological inhibition of Syk kinase inhibits tumor growth and promotes CD8+ T cell recruitment and activation.

A. Tumor volume of LLC inoculated subcutaneously in WT mice treated with 40 mg/kg R788 (n=6). **B.** Relative mRNA expression of TAMs from LLC tumors grown in WT animals and treated with R788. **p<0.01 and *p<0.05, t test **C**. FACS quantification of percentage of CD4+ and CD8+ T cells (gated on CD3+ T cells) in R788 treated LLC tumors (n=3, p<.05, t test). **D.** Flow cytometric representation of CD4+FoxP3+ regulatory T cells in the LLC tumors treated with R788. **E**. FACS analysis of CD44+CD62L- effector T cells (gated on CD8+ T cells) in R788 treated tumors (n=3), ** p<0.05, t test. **F**. *In vitro* tumor cell cytotoxicity induced by T cells isolated from R788 treated tumors (n=3), *** p<0.001, 2-way ANOVA using Bonferroni test.

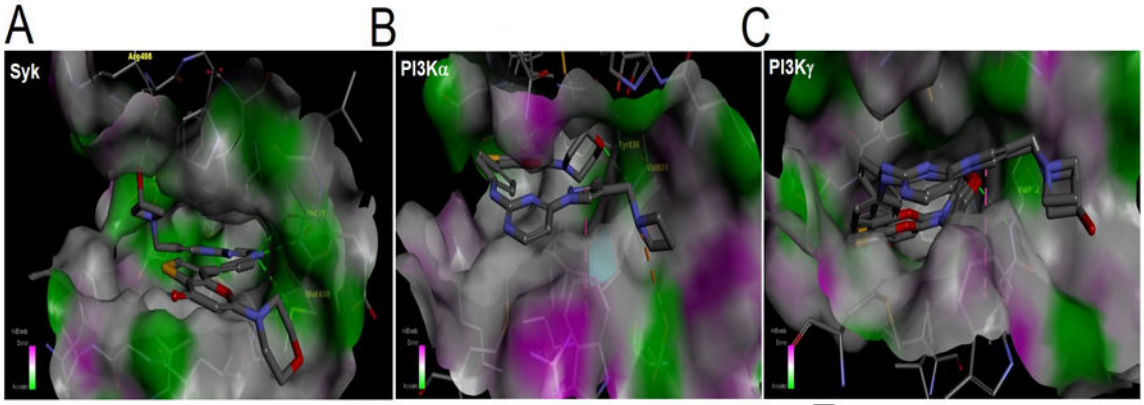

D

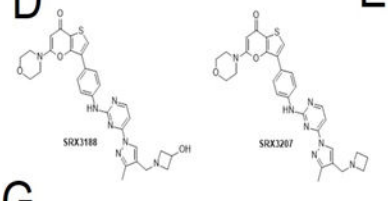

E

Compound	SYK (nM)	Zap70 (nM)	BRD41 (nM)	BRD42 (nM)	PI3K alpha (nM)	PI3K beta (nM)	PI3K delta (nM)	PI3K gamma (nM)
SRX3188	10.7	1300	>50000	No inhibition	861		1280	11100
SRX3207	39.9	31200	3070	3070	244		388	9790

F

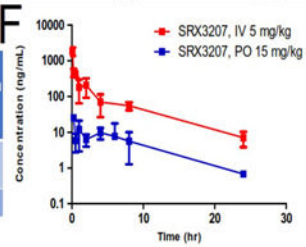

G

Route	Dosage (mg/kg)	Matrix	C0 (ng/mL)	T_{max} (hr)	C_{max} (ng/mL)	$T_{1/2}$ (hr)	MRT_{last} (hr)	MRT_{inf} (hr)	AUC_{last} (hr*ng/mL)	AUC_{inf} (hr*ng/mL)	Cl (mL/hr/kg)	Vss (mL/kg)	F (%)
IV	5	Plasma	3677	0.08	1865	5.84	3.92	4.78	1919	1978	2528	12086	
PO	15	Plasma		0.25	25.5	5.18	6.23	7.27	118	123			2.1%

Figure 5. ***In silico*** **design of dual Syk/PI3 kinase inhibitory chemotype.**

A-C. SRX3207 docked in the catalytic site of Syk kinase (A) or PI3Kα (B) or PI3Kγ (C).

D. Enzymatic inhibition profile (IC_{50}) of SRX3188 and SRX3207 against different targets.

E. Chemical structures of SRX3188 and SRX3207. **F-G.** Mean concentration time course of SRX3207 in mouse plasma (E) and pharmacokinetic parameters of SRX3207 in mouse (F) following 5mg/kg IV and 15 mg/kg PO administration.

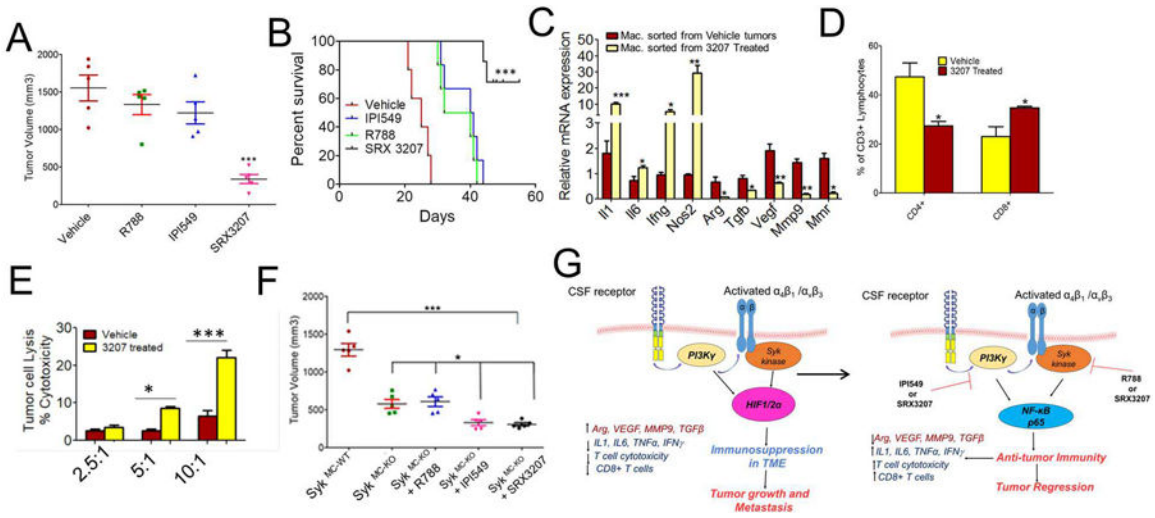

Figure 6. SRX3207 increases anti-tumor immune response.

A-B. Fig. shows tumor volume (A) and Kaplan Meir survival data (B) of LLC inoculated subcutaneously in WT mice and treated with 10 mg/Kg of R788, or IPI549 or SRX3207 (n=5, ***p<0.001, one-way ANOVA with Tukey's post hoc test). **C.** RTPCR analysis of cDNAs reflecting TAMs isolated from LLC tumors grown in WT animals and treated with SRX3207. ***p<0.001 **p<0.01 and *p<0.05, t test **D.** Quantification of CD4+ and CD8+ T cells in the LLC tumors treated with SRX3207 (n=3, *p<0.05, t test). **E.** *In vitro* tumor cell cytotoxicity induced by T cells isolated from SRX3207 treated tumors (n=3), 2-way ANOVA using Bonferroni test. **F.** Tumor volume of LLC tumors implanted in $Syk^{MC\text{-}KO}$ mice and treated with R788, IPI549 or SRX3207 data was analyzed by one-way ANOVA using Tukey's multiple comparison tests (n=5). **G.** Schematic representation of Syk, PI3Kγ, HIF1α axis in the control over tumor immunosuppression.